Electronic Supplementary Material (ESI) for Physical Chemistry Chemical Physics.

Supplementary Information:
Influence of Polar Co-Solutes and Salt on the Hydration of Lipid Membranes

Amanuel Wolde-Kidan,[1] Quoc Dat Pham,[2] Alexander Schlaich,[3]
Philip Loche,[1] Emma Sparr,[2] Roland Netz,[1] and Emanuel Schneck[4,*]

[1] *Fachbereich Physik, Freie Universität Berlin, Arnimallee 14, 14195 Berlin, Germany*
[2] *Division of Physical Chemistry, Chemistry Department,*
Lund University, P.O. Box 124, 22100 Lund, Sweden
[3] *Université Grenoble Alpes, CNRS, LIPhy, 38000 Grenoble, France*
[4] *Biomaterials Department, Max Planck Institute of Colloids and Interfaces, 14476 Potsdam, Germany*

(Dated: July 17, 2019)

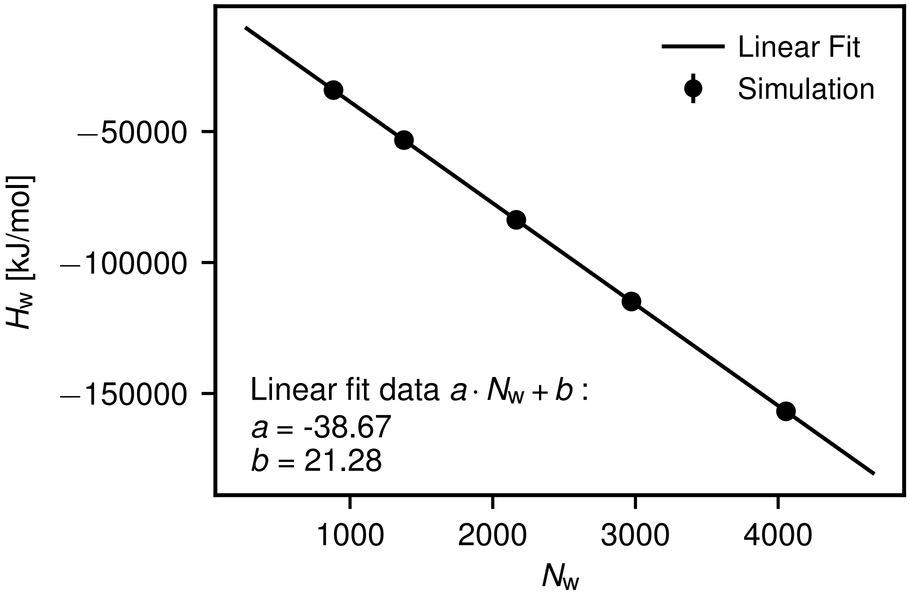

Supplementary Figure S1. Measured enthalpy from simulations of water boxes of different sizes. From a linear fit to the measured data, the partial enthalpy of water is determined to be $dH_{\mathrm{w}}/dN_{\mathrm{w}} = -38.67$ kJ/mol.

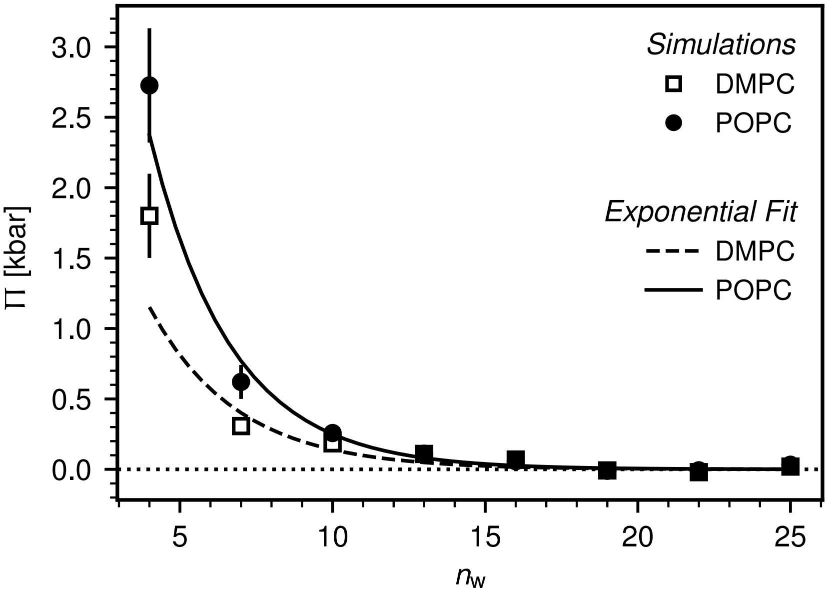

Supplementary Figure S2. Pressure distance curves obtained in simulations for the two lipids shown in a linear scale. The reference potential μ_0 was obtained by averaging results for the water chemical potential for which $n_{\mathrm{w}} > 19$ for simulations of DMPC and POPC. This is why only the average pressure for data points with $n_{\mathrm{w}} > 19$ goes to zero.

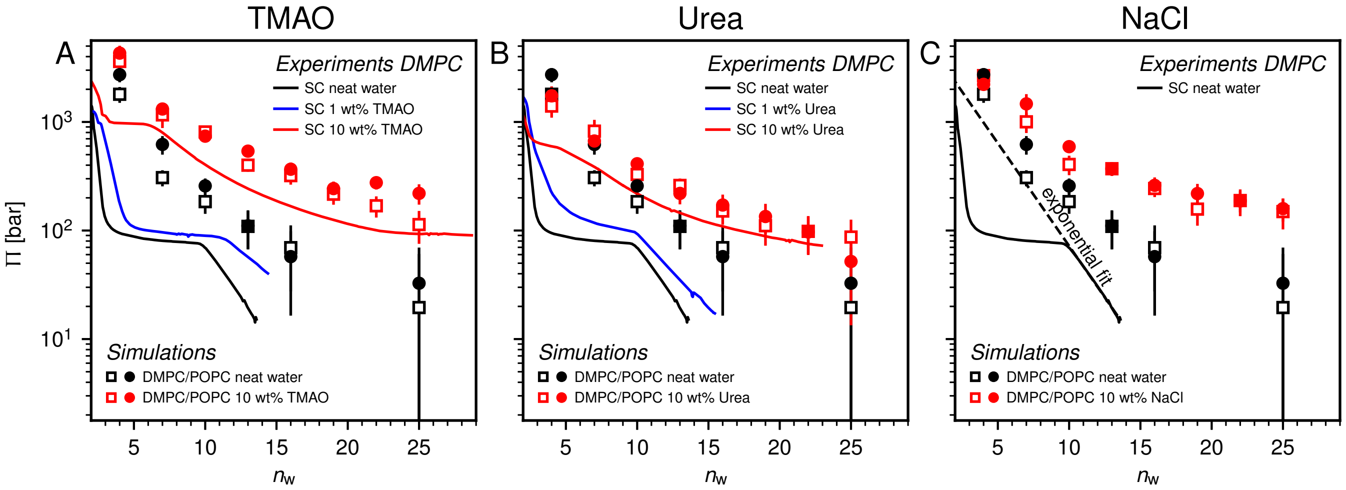

Supplementary Figure S3. Interaction pressure between membrane stacks in solution with TMAO (A), urea (B) and sodium chloride (C) from sorption calorimtetry (SC) experiments of DMPC lipids and simulations of DMPC and POPC. Panel C additionally includes an exponential fit to the experimental data for $n_{\mathrm{w}} > 10$. Comparison between experimental data and simulation results for DMPC bilayers shows larger deviations at low hydration levels. This is due to a phase transition from the fluid like to the gel like phase in the experiments when reaching a hydration level below $n_{\mathrm{w}} \approx 10$.

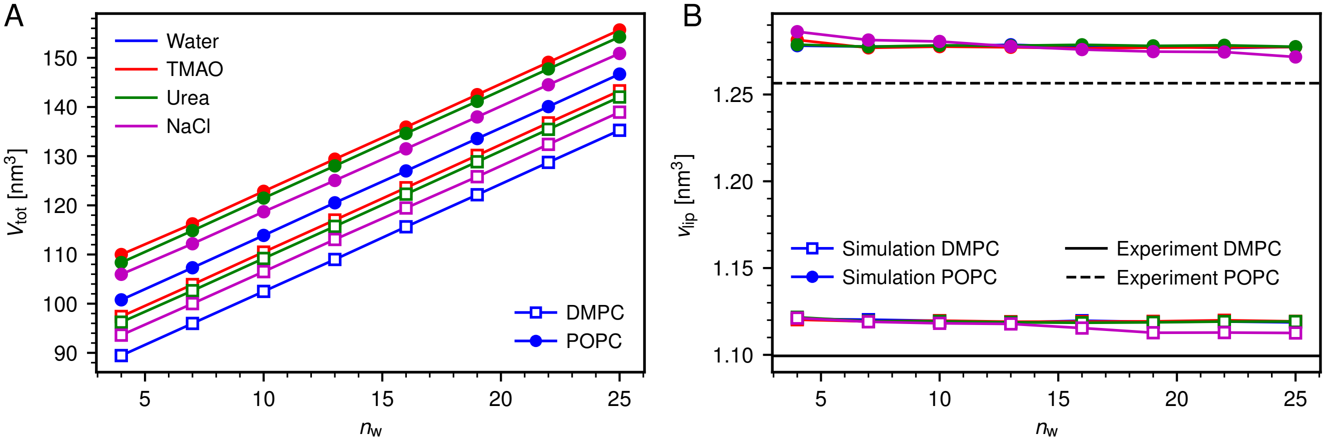

Supplementary Figure S4. Volumes from simulations of binary membrane-water-systems and ternary co-solute-membrane-water systems with 10 wt% of co-solutes. (A) Total system volume as a function of the hydration level. The decrease in system volume upon dehydration is constant for all simulated systems, suggesting a constant water partial volume v_{w}. (B) Average volume per lipid molecule for different hydration levels of membrane systems with and without 10 wt% of co-solutes. The lipid volume seems to remain constant during dehydration, while the area per lipid was observed to decrease (cf. Fig. 4 of the main text).

PARTIAL VOLUMES OF WATER AND LIPIDS

The slope of the total system volume V_{tot} as a function of the number of water molecules per lipid molecule $n_{\mathrm{w}} = N_{\mathrm{w}}/N_{\mathrm{lip}}$ remains constant for all observed systems (see Fig. S4A). This implies that the partial volume of water $v_{\mathrm{w}} = \partial V_{\mathrm{tot}}/\partial N_{\mathrm{w}}$ is unchanged in all simulations. Additionally, the volume per lipid molecule v_{lip} was computed from simulations as

$$v_{\mathrm{lip}} = \left(V_{\mathrm{tot}} - N_{\mathrm{w}} \cdot v_{\mathrm{w}} - N_{\mathrm{i}} \cdot v_{\mathrm{i}}\right) / N_{\mathrm{lip}}, \tag{S1}$$

where v_{i} denotes the partial volume of the respective co-solutes and N_{i} is the number of co-solute molecules in the simulation. The partial volume of the specific co-solute was estimated by the volume increase between simulations with 1wt% and 10wt% of the co-solute at the same hydration level as $v_{\mathrm{i}} \approx \Delta V_{\mathrm{tot}}/\Delta N_{\mathrm{i}}$.

Like the water partial volume, the lipid partial volume appears to remain constant throughout all simulation setups (see Fig. S4B). Since the lipid area A_{lip} was found to be affected by hydration and addition of co-solutes (see main text), this suggests an elongation or contraction of the lipids along their axis, depending on the change in A_{lip}. A difference of about 3-4% is observed between values for the lipid volumes measured in our simulations and values obtained experimentally using the neutral flotation method [1]. This discrepancy might be due to forcefield limitations.

RELATION BETWEEN OSMOTIC COEFFICIENTS AND ACTIVITY COEFFICIENTS

When using the definition of the osmotic coefficient Φ in equation (1) in the main text, one can express the water chemical potential μ_w in solution with a solute as

$$\mu_\mathrm{w} = \Phi RT\ \ln(x_\mathrm{w}) = -\Phi RT\ \ln(1 + M_\mathrm{w} b) \approx -\Phi RT M_\mathrm{w} b, \tag{S2}$$

where M_w is the water molar mass and b is the molal concentration of the solute. The solute chemical potential μ_s is given by

$$\mu_\mathrm{s} = RT \ln(\gamma b), \tag{S3}$$

with the solute specific activity coefficient γ. The Gibbs-Duhem equation at constant pressure and temperature as a function of the solute molality results in the relation

$$b M_\mathrm{w} \mathrm{d}\mu_\mathrm{s} = -\mathrm{d}\mu_\mathrm{w}. \tag{S4}$$

Using equations (S2) and (S3) we can write the total differentials of μ_s and μ_w as

$$\mathrm{d}\mu_\mathrm{w} = -RT M_\mathrm{w} b\ \mathrm{d}\Phi - \Phi RT M_\mathrm{w}\ \mathrm{d}b \tag{S5a}$$

$$\mathrm{d}\mu_\mathrm{s} = \frac{RT}{\gamma}\ \mathrm{d}\gamma + \frac{RT}{b}\ \mathrm{d}b. \tag{S5b}$$

Now substituting equations (S5) into equation (S4) we obtain

$$b \mathrm{d}\ln(\gamma) + \mathrm{d}b = \mathrm{d}(\Phi b). \tag{S6}$$

Solving equation (S6) for $\mathrm{d}\ln(\gamma)$ and integrating then leads to the relation between activity coefficient and osmotic coefficient referred to in the main text

$$\ln(\gamma) = \Phi - 1 + \int_0^b \frac{\Phi - 1}{b'}\ \mathrm{d}b'. \tag{S7}$$

OSMOTIC COEFFICIENTS FOR TMAO

In order to obtain the osmotic coefficient of TMAO solutions at different concentrations $\Phi_{\mathrm{TMAO}}(x_{\mathrm{w}})$, the dependence of the water activity on the TMAO molality reported in reference [2] was used. For this, the relation between solute molality and water mole fraction $b(x_{\mathrm{w}}) = (x_{\mathrm{w}}^{-1} - 1)/M_{\mathrm{w}}\nu$, where additionally $\nu_{\mathrm{TMAO}} = 1$ was then substituted.

Together with equation (1) from the main text this then yields the following expression

$$\Phi_{\mathrm{TMAO}}(x_{\mathrm{w}}) = \frac{M_{\mathrm{w}}(b(x_{\mathrm{w}}) + Ab(x_{\mathrm{w}})^2)}{\ln(x_{\mathrm{w}})}, \tag{S8}$$

where $A = 0.18$ was obtained in reference [2] based on a quadratic fit to the water activity data. Equation (S8) was then used to compute the TMAO osmotic coefficients for the augmented model in equation (7) of the main text.

OSMOTIC COEFFICIENTS FOR UREA AND SODIUM CHLORIDE

For urea and sodium chloride, previously determined dependencies of the respective osmotic coefficients on the cosolute molality were obtained from the literature. These expressions were then transformed from the molality scale to the mole fraction scale using the relation $b(x_{\mathrm{w}})$ from above. Note that $\nu_{\mathrm{NaCl}} = 2$. Additionally, the pre-factor $K = (x_{\mathrm{w}}^{-1} - 1)/\ln(x_{\mathrm{w}}^{-1})$ is introduced to account for the different reference potential used in the definition of the molality based osmotic coefficient $\Phi_{\mathrm{b}}(b) = \Delta\mu/RT\nu M_{\mathrm{w}}b$. This definition was used in the references, whereas in this work we use the fractional osmotic coefficient $\Phi(x_{\mathrm{w}})$ as defined in equation (1) of the main text.
At $T = 25°C$ the relation reported in reference [3] leads to the following expression for the osmotic coefficient of an urea-water-solution

$$\Phi_{\mathrm{urea}}(x_{\mathrm{w}}) = K\left(1 - \frac{c_1 b(x_{\mathrm{w}})}{1 + c_2 b(x_{\mathrm{w}})} - \frac{c_3 b(x_{\mathrm{w}})^2}{(1 + c_2 b(x_{\mathrm{w}}))^2}\right), \tag{S9}$$

where values of $c_1 = 0.042783$, $c_2 = 0.15$ and $c_3 = 0.0004198$ were found in reference [3] to reproduce the osmotic coefficient correctly up to $b = 20$ mol/kg corresponding to $x_{\mathrm{w}} \approx 0.74$.

For sodium chloride, osmotic coefficients were computed using the following relation based on the findings of reference [4]

$$\begin{aligned}\Phi_{\mathrm{NaCl}}(x_{\mathrm{w}}) = K\Bigg(1 - \frac{S_f\sqrt{d_0}}{A^3 b(x_{\mathrm{w}})}\left[1 + A\sqrt{b(x_{\mathrm{w}})} - 2\ln(1 + A\sqrt{b(x_{\mathrm{w}})}) - \frac{1}{1 + A\sqrt{b(x_{\mathrm{w}})}}\right]\\ + Bb(x_{\mathrm{w}}) + Cb(x_{\mathrm{w}})^2 + Db(x_{\mathrm{w}})^3\Bigg),\end{aligned} \tag{S10}$$

where at $T = 25°C$ the following values of $S_f\sqrt{d_0} = 1.1705$, $A = 1.3924$, $B = 2.655 \cdot 10^{-2}$, $C = 9.60 \cdot 10^{-3}$ and $D = -0.96 \cdot 10^{-3}$ are reported. The derivation of equation (S10) is based on the Debye-Hückel limiting law for the activity coefficient, which is then transformed to the osmotic coefficient using equation (S7) [4].

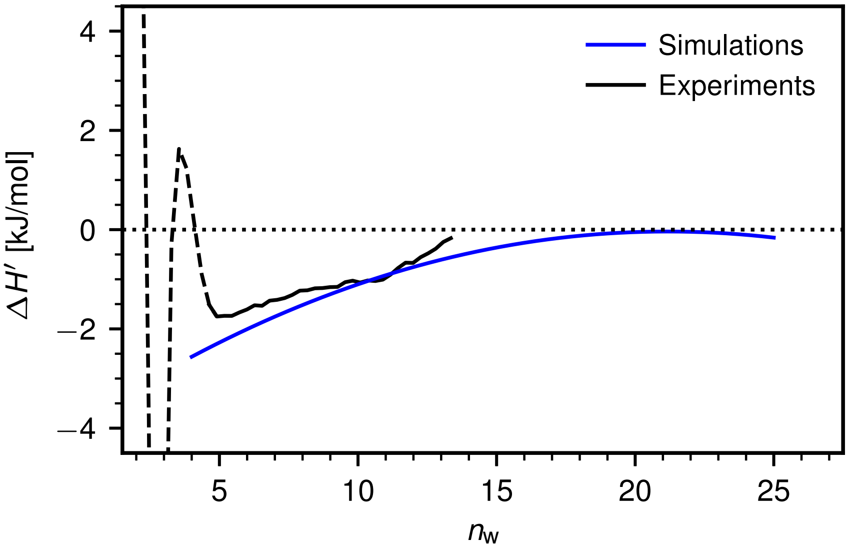

Supplementary Figure S5. Comparison between differential enthalpies $\Delta H' = H'_{5\mathrm{wt\%\ TMAO}} - H'_{\mathrm{water}}$ (see main text) from sorption calorimetry experiments and MD simulations of POPC lipids. The difference between the differential enthalpies obtained in setups with 5 wt% TMAO and pure water was computed at the same hydration level n_w. Dashed lines indicate regimes where TMAO forms a separate phase and POPC undergoes a phase transition in experiments.

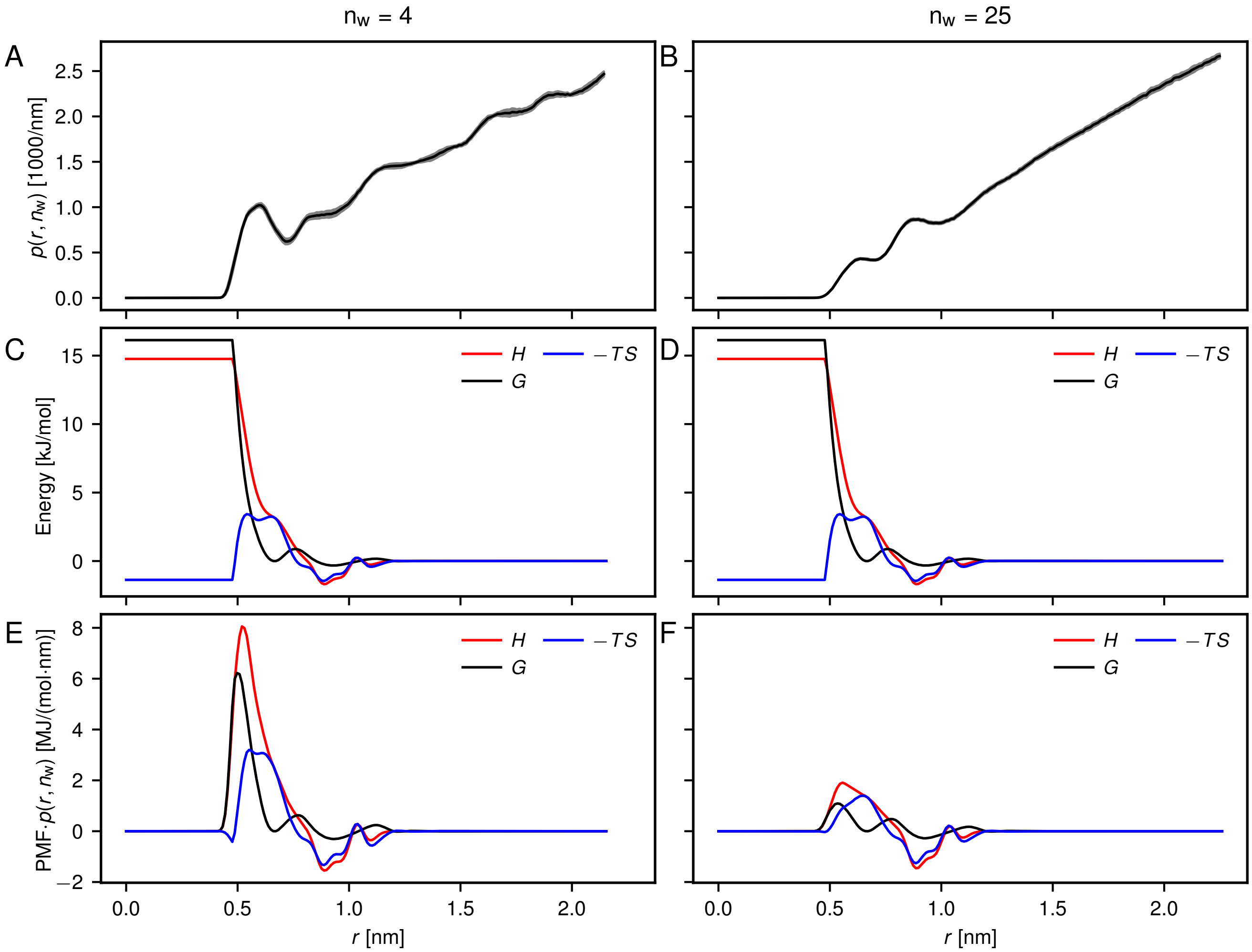

Supplementary Figure S6. Details for the computation of the linear combination of the water-membrane and water-TMAO systems for DMPC, shown exemplary for two hydration levels $n_\mathrm{w} = 4$ and $n_\mathrm{w} = 25$. (A-B) Normalized distribution of TMAO-TMAO separations as observed in DMPC simulations with 10 wt% of TMAO. Data are averaged over five independent simulations and the standard error is indicated as the area shaded in grey. (C-D) Potential of mean force for TMAO in water as reported in reference [5]. For separations below the smallest measured value, the PMF was taken to be constant. (E-F) Product of respective PMF components and TMAO-TMAO separation distribution, which was then used to compute the theoretical contributions of pairwise TMAO-TMAO interactions to the free energy of the TMAO loaded membranes (see equations (9) of the main text).

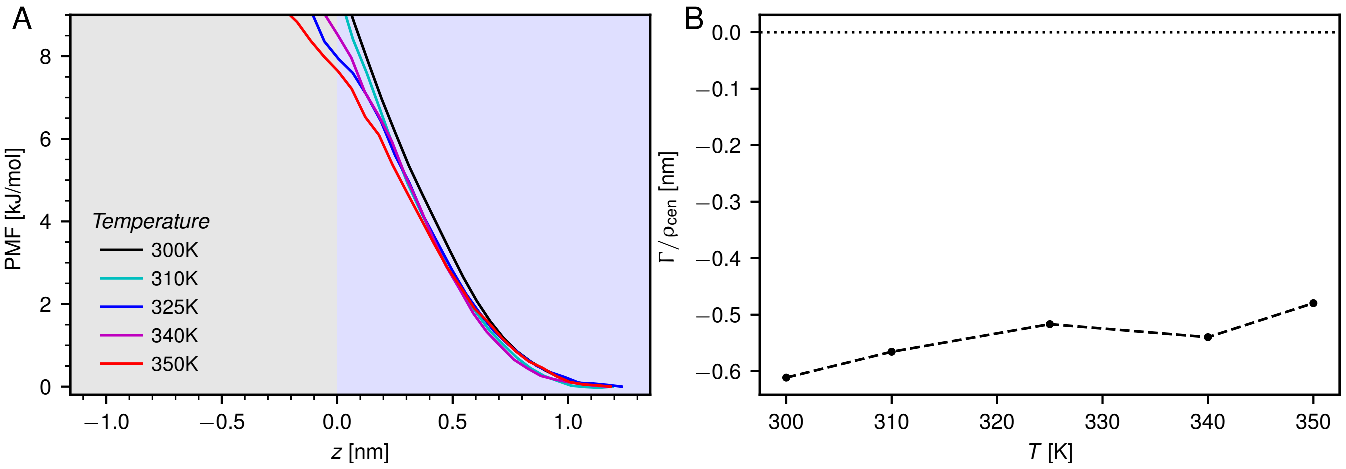

Supplementary Figure S7. (A) Potential of mean force (PMF) between the DMPC lipid interface and TMAO molecules at different temperatures. The DMPC-TMAO PMF was estimated from density profiles $\rho_{\mathrm{TMAO}}(z)$ obtained from simulations with 1wt% of TMAO, by using the identity $\mathrm{PMF}(z) = -k_{\mathrm{B}}T\ln(\rho(z)/\rho_{\mathrm{cen}})$. (B) Temperature dependent surface excess of TMAO at the DMPC interface from simulations with 1wt% of TMAO. The computation of Γ was performed as defined in Eq. (4) in the main text. Assuming temperature-independent enthalpic and entropic contributions, the decreasing repulsion with increasing temperature indicates entropic attraction over-compensated by enthalpic repulsion. Similarly, a decreasing range of the repulsion between co-solutes and surfaces has previously been associated with enthalpy-driven depletion forces. [6].

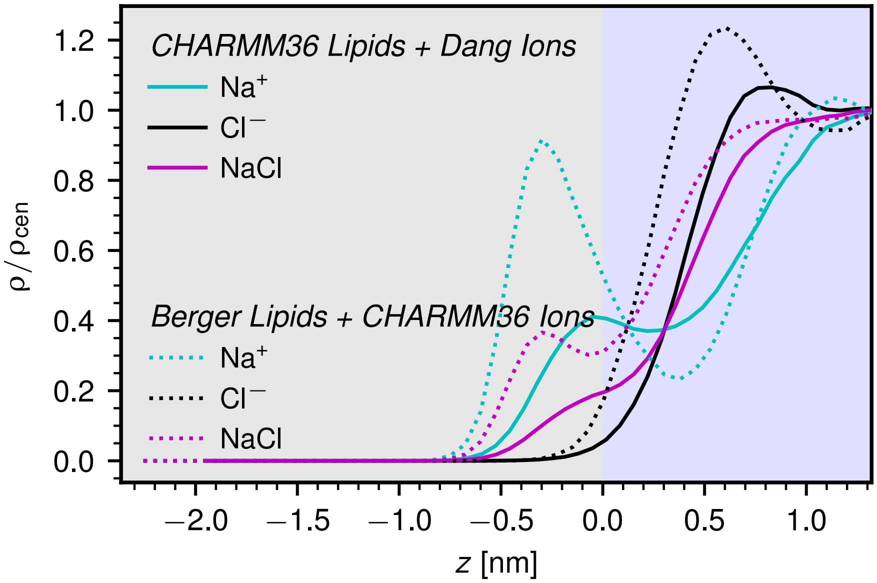

Supplementary Figure S8. In order to evaluate the relative importance of the ion and the lipid forcefields regarding the observed Na^+ adsorption to the membrane surfaces, two different forcefield setups were analyzed. The CHARMM36 forcefield for the lipids [7] in combination with the Dang NaCl forcefield [8] together with the TIP3P water model [9, 10] on the one side are compared to a Berger lipid [11] and CHARMM36 NaCl system [12] in SPC/E water [13] on the other side. We find that regardless of the NaCl forcefield used (Dang or CHARMM36) the Na^+ adsorption is much stronger for the Berger lipids, compared to the CHARMM36 lipids.

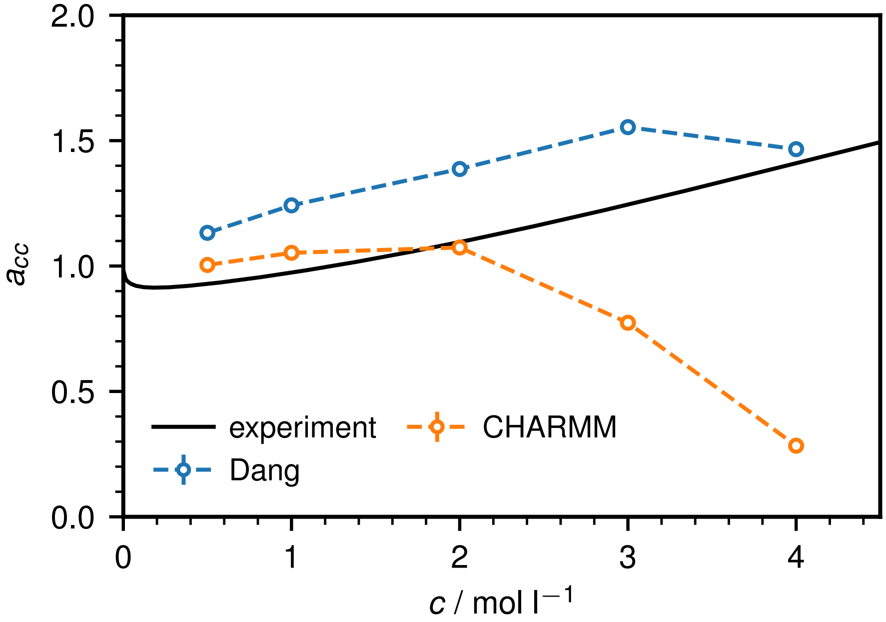

Supplementary Figure S9. Comparison of the logarithmic derivative $a_{\mathrm{cc}} := dln(\gamma)/dc$ of the activity coefficient between the CHARMM36 [12] and Dang NaCl [8] forcefield in bulk water (employing the TIP3P [9, 10] and SPC/E [13] water model respectively). It is apparent that the Dang forcefield reproduces the experimental activity coefficient better than the CHARMM36 forcefield, especially at concentrations $c > 2$ mol/l.

---

[*] Email: schneck@mpikg.mpg.de

[1] A. I. Greenwood, S. Tristram-Nagle, and J. F. Nagle, Chemistry and Physics of Lipids **143**, 1 (2006).
[2] E. S. Courtenay, M. W. Capp, C. F. Anderson, and M. T. Record, Biochemistry **39**, 4455 (2000).
[3] R. H. Stokes, Australian Journal of Chemistry **20**, 2087 (1967).
[4] A. R. G. Lang, Australian Journal of Chemistry **20**, 2017 (1967).
[5] E. Schneck, D. Horinek, and R. R. Netz, Journal of Physical Chemistry B **117**, 8310 (2013).
[6] L. Sapir and D. Harries, Current Opinion in Colloid and Interface Science **20**, 3 (2015).
[7] J. B. Klauda, R. M. Venable, J. A. Freites, J. W. O'Connor, D. J. Tobias, C. Mondragon-Ramirez, I. Vorobyov, A. D. MacKerell, and R. W. Pastor, Journal of Physical Chemistry B **114**, 7830 (2010).
[8] L. X. Dang, Journal of the American Chemical Society **117**, 6954 (1995).
[9] W. L. Jorgensen, J. Chandrasekhar, J. D. Madura, R. W. Impey, and M. L. Klein, The Journal of Chemical Physics **79**, 926 (1983).
[10] S. R. Durell, B. R. Brooks, and A. Ben-Naim, Journal of Physical Chemistry **98**, 2198 (1994).
[11] O. Berger, O. Edholm, and F. Jähnig, Biophysical Journal **72**, 2002 (1997).
[12] R. M. Venable, Y. Luo, K. Gawrisch, B. Roux, and R. W. Pastor, Journal of Physical Chemistry B **117**, 10183 (2013).
[13] H. J. C. Berendsen, J. R. Grigera, and T. P. Straatsma, The Journal of Physical Chemistry **91**, 6269 (1987).